Active control of road booming noise in automotive interiors

Shi-Hwan Oh,[a] Hyoun-suk Kim,[b] and Youngjin Park
Center for Noise and Vibration Control (NOVIC), Department of Mechanical Engineering, Korea Advanced Institute of Science and Technology (KAIST), Science Town, Taejon 305-701, Korea

(Received 13 August 2000; revised 19 September 2001; accepted 27 September 2001)

An active feedforward control system has been developed to reduce the road booming noise that has strong nonlinear characteristics. Four acceleration transducers were attached to the suspension system to detect reference vibration and two loudspeakers were used to attenuate the noise near the headrests of two front seats. A leaky constraint multiple filtered-X LMS algorithm with an IIR-based filter that has fast convergence speed and frequency selective controllability was proposed to increase the control efficiency in computing power and memory usage. During the test drive on the rough asphalt and turtle-back road at a constant speed of 60 km/h, we were able to achieve a reduction of around 6 dB of *A*-weighted sound pressure level in the road booming noise range with the proposed algorithm, which could not be obtained with the conventional multiple filtered-X LMS algorithm. © *2002 Acoustical Society of America.* [DOI: 10.1121/1.1420390]

PACS numbers: 43.50.Ki, 43.50.Lj [MRS]

I. INTRODUCTION

Active noise and vibration control with feedforward strategy[1–3] has been widely used in several practical applications such as the engine or exhaust noise control in passenger vehicles, passenger ships, turbo machinery, aircraft and vibration isolation systems.[4–11] One of the most difficult applications in which to implement active control is road booming noise attenuation[12–16] because of the nonlinear characteristics of road data and sensitivity of the transducer location on the control performance. Several studies[17–20] were carried out to estimate the control performance and select the location of reference transducer, error microphone, and loudspeakers for better performance in road-noise control. Because the road-noise characteristic is much different from one car to another and the transfer path from the tire to interior acoustics is complicated, the location of transducers for optimal reduction of noise and the expected reduction cannot be generalized for passenger vehicles. Road booming noise also has nonstationary characteristics caused by various road profiles and the change of driving speeds.

This paper sets out a strategy for attenuation of the road booming noise of a specific mid-size passenger vehicle with a 2000 cc engine; selection of the location and number of reference signals, appropriate positioning of control speakers, development of an efficient control algorithm for the experiment. Reference transducers and control speakers were optimally positioned by the experimental estimate of control performance using the multiple coherence function. An effective control algorithm is also developed to concentrate the control effort on the booming noise frequency band and increase the convergence speed. The hardware-in-the-loop simulation and experimental result are presented and the proposed control algorithm is compared with the conventional (constraint) filtered-X LMS algorithm through the simulation and experiment.

II. CHARACTERISTICS OF ROAD BOOMING NOISE

The nonstationary vibrations of front and rear wheels are generated by nonuniform road profiles and the change of vehicle speed. They propagate though the tire and complicated suspension system and finally generate structure-borne noise, impulsive noise, and other low frequency noise in the interior of the passenger vehicle. These noises lead to acoustical resonances in the interior of the passenger car and such resonant noise is called ''road booming noise.'' There are several characteristics of road booming noise. First, the independent vibrations of four wheels generate it. So, it is hardly reduced by ANC with just one or two reference sensors. Second, the properties of road booming noise change continuously as the vehicle speed or road profile varies. The system from the wheel vibration to road booming noise is not linear because of the complexity of suspension system, transfer path, and the nonlinear interaction between vibration and sound, etc. It causes the road booming noise characteristics of each vehicle to be distinctive. Thus, the active control of road booming noise in the actual road test is rather difficult to achieve than the control in the laboratory setup.

The sound pressures of various road booming noises were detected from the microphone near the driver's headrest inside the vehicle while driven over some road profiles at several different speeds and its spectrum is shown in Fig. 1. No sports wheels were fitted. Four standard tires were attached to the test vehicle. It is hard to recognize the characteristics of booming noise from the original spectrum, but after *A*-weighting, the road booming noise component appears at around 250 Hz. On turtle-back, concrete, and rough asphalt roads at various vehicle speeds, the peak near 250 Hz did not change while those of other low frequencies were shifted. The undesired noise was influenced by the cavity mode behavior of the test vehicle. ''Booming'' indicates that

[a]Present address: Department of Satellite Control System, Satellite Division, Korea Aerospace Research Institute (KARI), P.O. Box 113, Yusung, Taejon 305-600, Korea; electronic mail: oshysh@kari.re.kr
[b]Present address: CTO, Digital Contents Laboratory, Emersys Corp., 404.KIPA, 48 Jang-Dong Yusung-Gu, Daejon 305-301, Korea.

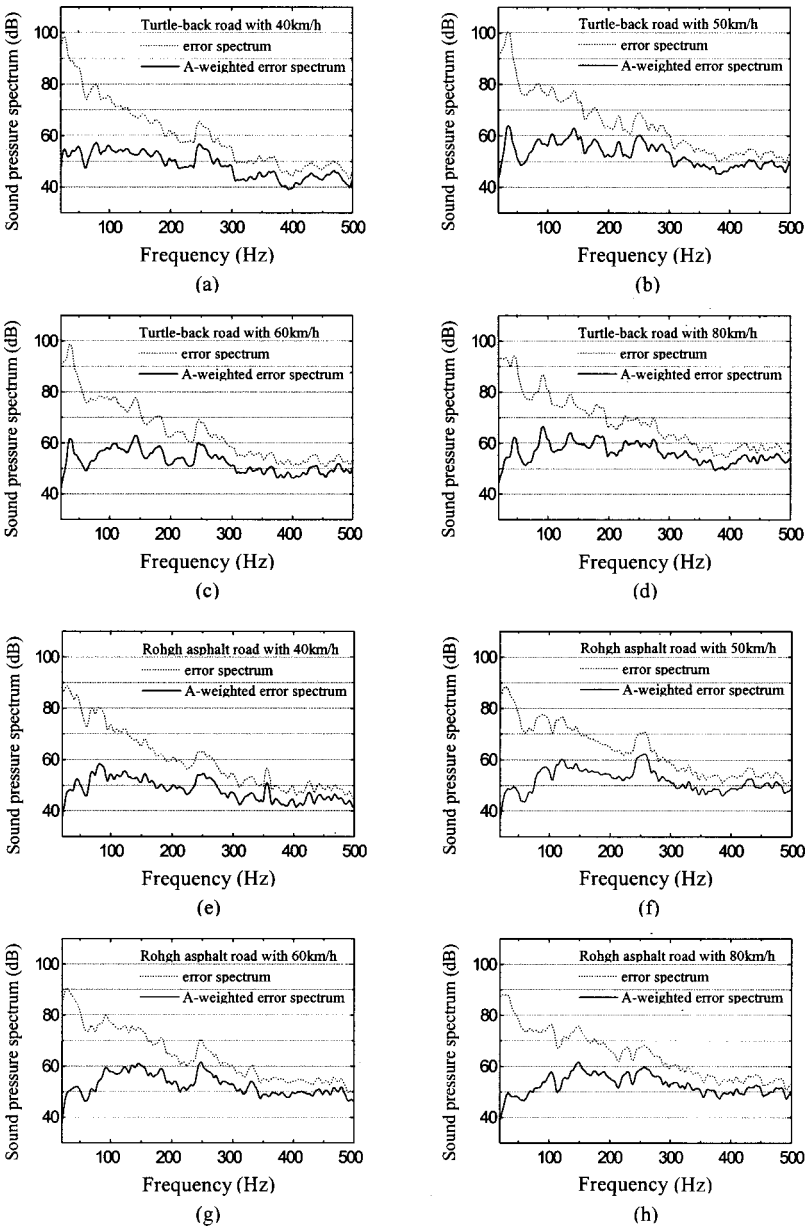

FIG. 1. The characteristics of road booming noise (*A*-weighted) sound pressure level inside the test vehicle driving a turtle-back road with (a) 40, (b) 50, (c) 60, and (d) 80 km/h, respectively, rough asphalt road with (e) 40, (f) 50, (g) 60, and (h) 80 km/h, respectively.

the noise is structure-borne. We did not test the correlation between the booming noise and the internal tire resonance.

III. SELECTION OF REFERENCE SIGNALS AND POSITIONING OF LOUDSPEAKERS

In order to select a set of reference transducers that offers the largest potential sound pressure level reduction, the multiple coherence method is generally used.[21] From the multiple coherence function, the incoherent output can be estimated as

$$S_{nn}(f)=(1-\gamma_{xy}^2(f))S_{yy}(f), \tag{1}$$

where S_{nn} is the incoherent output, γ_{xy}^2 is the multiple coherence function between the input and output, and S_{yy} is the uncontrolled output spectrum. The incoherent output is the sound pressure level at the error microphone that is not coherent with the input transducer. Therefore, the incoherent output can be used to determine the maximum reduction in sound pressure level a particular set of input transducers is capable of achieving. The maximum potential noise reduction in decibels is

$$\mathrm{NR}=-10\log(1-\gamma_{xy}^2(f)). \tag{2}$$

Road tests with various vehicles have shown that the ordinary coherence is often poor, less than 30%, between the signals from each individual accelerometer attached to the structure and the interior sound pressure signals. Several studies[14–20] had already used multiple reference signals to increase the coherence.

In order to determine the location and number of reference transducers to get a satisfactory reduction level of road booming noise for the passenger car, the following experiment was performed. Before the experiment, we selected sixteen possible candidates for a set of accelerometer locations in the suspension system, as shown in Fig. 2. The eight possible locations for the front and rear suspensions are symmetric. First, we got an error signal from a microphone placed on the driver's headrest and three acceleration signals from a

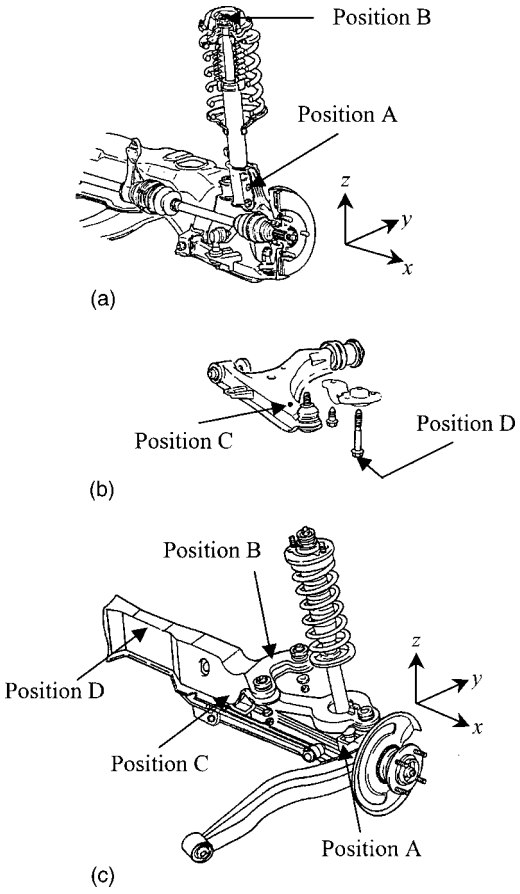

FIG. 2. Accelerometer locations: (a) front right suspension system (symmetric with front left); (b) lower arm of front right suspension system (symmetric with front left); (c) rear right suspension system (symmetric with rear left).

triaxial accelerometer attached to each candidate location while driving on the asphalt road at a constant speed of 60 km/h. The maximum possible reduction level for each reference candidate is listed in Table I. The result shows that it is hard to attenuate the road booming noise over 3 dB with only one triaxial accelerometer. Thus, by using four triaxial accelerometers, we got twelve reference signals and a microphone signal driving under the same condition. The accelerometers were located at position C for the front right and left suspension system and position A for the rear system on which it was easy to attach the sensors because the maximum reduction level for each position was similar. Multiple coherence functions were calculated for several combinations of acceleration signals and Fig. 3 shows the results. Because of the limited calculation power in real-time control process, the number of reference signals was limited to six. Comparing the results, it was found that the maximum attenuation of about 6 dB of the road booming noise band could be achieved with the front right and left acceleration signals (six channels). The front sound field was hardly correlated to the rear acceleration signals but to the front signals only in the booming frequency range, and the rear sound field was correlated to the rear signals only. From this experiment, for the case of a passenger car, an efficient positioning of six reference signals was decided on the two lower arms of the front wheels. The accelerometer signals for reference selection were not measured for turtle-back road drives because the booming noise for turtle-back road has particular frequency components, which are proportional to the vehicle speed under 200 Hz and do not appear for other roads. The reference locations determined by the coherence test for the turtle-back road may not be adequate for the general road condition.

Because the noise reduction level and convergence parameter of the LMS-based algorithm are affected by the secondary paths,[22] the appropriate positioning of loudspeakers was also determined using the measured reference and error microphone signals, which contain the primary and secondary path information.[23] Figure 4 shows the experimental setup to determine the loudspeaker position. The road booming noise control system can be written as

$$\mathbf{E}(f)=\mathbf{A}(f)+\mathbf{B}(f)\mathbf{W}(f), \tag{3}$$

where $\mathbf{E}(f)$ is an error vector in frequency domain, $\mathbf{A}(f)$ is the road booming noise, $\mathbf{B}(f)$ is a filtered reference, and $\mathbf{W}(f)$ is an adaptive filter. The information of transfer functions between the control speakers and error microphone is included in $\mathbf{B}(f)$, which depends on the speaker positions. The transfer functions were estimated for positions A, B, and C off-line. For each set of speaker locations, we calculated the optimum solutions of $\mathbf{W}(f)$ and the expected noise reduction levels from Eq. (3). The six accelerometers determined from the reference selection were used in the determination of speaker locations. Consequently, around 5–6 dB reduction could be expected when the speaker was located at the bottom behind the two front seats, i.e., position B.

IV. CONTROL ALGORITHMS

A. Leaky constraint multiple filtered-X LMS (CMFX LMS) algorithm

A *filtered-x* LMS (FX) LMS algorithm has been widely used in control applications. It is well known that the delay in the secondary path decreases the upper limit of convergence coefficient in this algorithm, so it is not as fast as an LMS algorithm in convergence of adaptive filter to the optimal solution. In order to reduce nonstationary signals effectively, a fast convergent algorithm is needed to track the

TABLE I. Maximum averaged reduction levels using one triaxial accelerometer.

Front left		Front right		Rear left		Rear right	
Position	NR (dB)	Position	NR (dB)	Position	NR (dB)	Position	NR (dB)
A	2.68	A	2.43	A	2.24	A	2.13
B	2.92	B	2.32	B	2.65	B	2.75
C	2.64	C	2.55	C	2.24	C	2.46
D	2.97	D	2.93	D	2.90	D	3.79

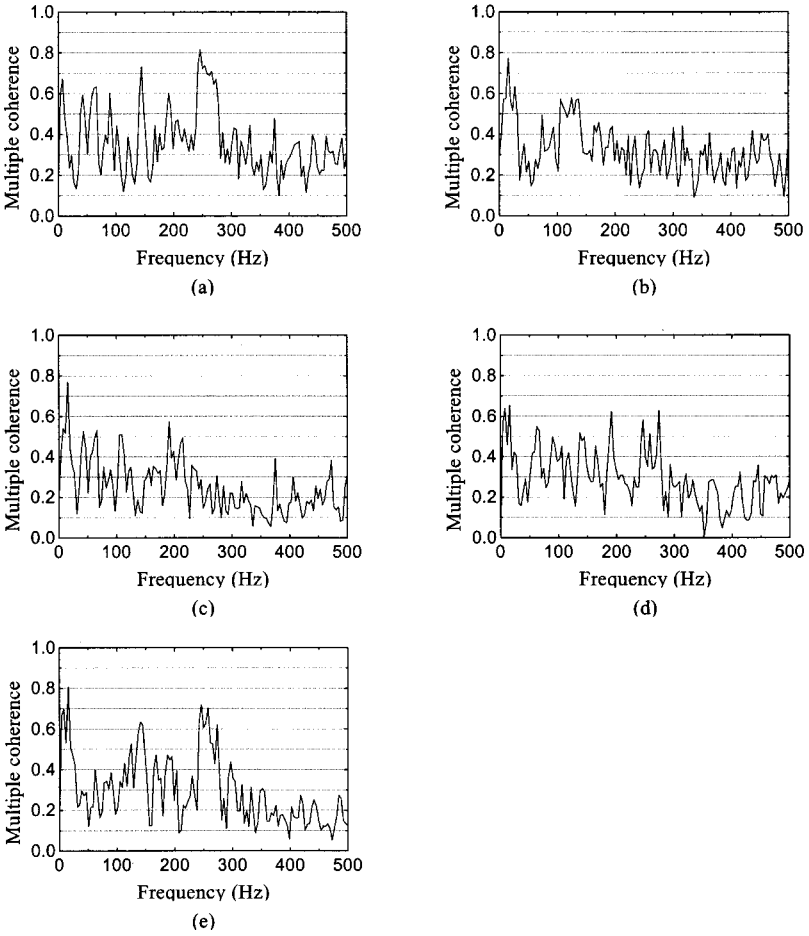

FIG. 3. Multiple coherence function between the error microphone and (a) front accelerometer signals (six channels; right and left *x, y, z* directions at front position C), (b) rear accelerometer signals (six channels; right and left *x, y, z* directions at rear position A), (c) four *x*-direction signals (four *x* directions at front position C and rear position A), (d) four *y*-direction signals (four *y* directions at front position C and rear position A), and (e) four *z*-direction signals (two *z* directions at front position C and rear position A).

undesired noise. In 1992 and 1994, a constraint *filtered-x* LMS (CFX LMS) algorithm, which has a convergence behavior similar to the LMS algorithm, was proposed by Bjarnason[24] and Kim[25] independently. It uses the constraint error instead of the error signal so that the time invariant assumption in the *filtered-x* LMS algorithm is not needed. Consequently, in the presence of a secondary path, the CFX LMS algorithm[26,27] recovers the upper limit of convergence coefficient that had been lowered by the delay in the secondary path.

In order to attenuate the road booming noise with a CFX LMS algorithm, it is necessary to extend the algorithm for a system with N references, K control speakers, and M error microphones. The mth error $e_m(k)$ and constraint error $e'_m(k)$ are expressed as

$$e_m(k)=d_m(k)+\sum_{n=1}^{N}\sum_{k=1}^{K}\sum_{j=0}^{L_h}\sum_{i=0}^{L} h_{mkj}w_{kni}(k-j)\times x_n(k-i-j), \tag{4}$$

$$e'_m(k)=d_m(k)+\sum_{n=1}^{N}\sum_{k=1}^{K}\sum_{j=0}^{L_h}\sum_{i=0}^{L} h_{mkj}w_{kni}(k)\times x_n(k-i-j), \tag{5}$$

where $d_m(k)$ is the undesired noise signal at the mth microphone, $x_n(k)$ is the nth reference, w_{kni} is the ith coefficient of the FIR-type adaptive filter $W_{kn}(z)$, i.e., $W_{kn}(z)=\Sigma_{i=0}^{i=L}w_{kni}(k)z^{-i}$ whose input is the nth reference and whose output goes to the kth control speaker, and h_{mkj} is the jth coefficient of the secondary path $H_{mk}(z)$, i.e., $H_{mk}(z)=\Sigma_{j=1}^{j=L_h}h_{mkj}z^{-j}$, which is located between the kth control speaker and the mth error microphone. The constraint error $e'_m(k)$ can be calculated by modifying $e_m(k)$ by eliminating $d_m(k)$ from Eqs. (4) and (5).

The weights in the CMFX LMS algorithm are updated by the steepest descent method. Derivation of the CMFX LMS algorithm that tries to minimize the cost function $e'^2_1(k)+e'^2_2(k)+\cdots+e'^2_M(k)$ is straightforward. To increase the stability bound and tracking performance, a leakage factor[28] was added in the update algorithm. The leaky CMFX LMS algorithm is summarized in Table II. The signal $fx_{mkn}(k)$ is a filtered signal of $x_n(k)$ through the error path

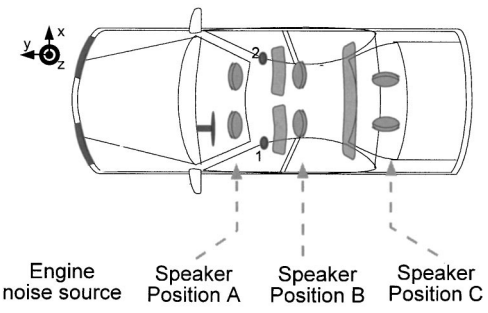

FIG. 4. Experimental setup to determine the position of the loudspeaker.

TABLE II. Summary of leaky CMFX LMS algorithm.

Given $x_n(k), e_m(k), \quad n=1,2,...,N, \quad m=1,2,...,M$ at k step

$$fx_{mkn}(k)=\sum_{j=0}^{L_h} h_{mkj}x_n(k-j)$$

$$e'_m(k)=e_m(k)-\sum_{k=1}^{K}\sum_{j=0}^{L_h} h_{mkj}y_k(k-j)+\sum_{n=1}^{N}\sum_{k=1}^{K}\sum_{i=0}^{L} w_{kni}(k)fx_{mkn}(k-i)$$

$$w_{kni}(k+1)=(1-\alpha)w_{kni}(k)-2\mu\sum_{m=1}^{M} e'_m(k)fx_{mkn}(k-i)$$

$$y_k(k)=\sum_{n=1}^{N}\sum_{i=0}^{L} w_{kni}(k)x_n(k-i)$$

model $H_{mk}(z)$. The CMFX LMS algorithm is different from the MFX LMS algorithm only in that it uses $e'_m(k)$ instead of $e_m(k)$.

B. Leaky CMFX LMS algorithm with an IIR-based filter

When an FIR structure is used for an adaptive filter in active noise control, it needs a sufficiently large number of filter weights to achieve satisfactory control performance, especially for a lightly damped system. Using an IIR structure with a smaller number of weights can reduce the necessary computation power; however it may have instability or nonlinearity problems on updating the filter weights. In order to avoid these problems, an IIR-based filter,[29,30] which is a linear combination of fixed stable IIR filters, was proposed.

The selection of IIR bases is very important in a system-identification point of view. First, we need to consider the orthogonality between IIR bases, which means the impulse responses of IIR filter bases are orthogonal to each other. Otherwise, each weight of an IIR-based filter gives undesirable coupling effects in the updating process. If each IIR filter base has its own dominant frequency range, it is possible to control the undesired noise only in the selected frequency range. We can select the control frequency range by using these IIR filter bases appropriately. To get a decaying impulse response, exponential sine or cosine functions having their own dominant frequencies are considered as the impulse responses of an IIR filter base. These functions are not exactly orthogonal to each other, but approximately orthogonal if damping is small. We chose two elementary IIR filter bases as follows:

$$B_{i,c}(z)=\frac{1-e^{-\sigma_i T}Z^{-1}\cos\omega_i T}{1-2e^{-\sigma_i T}z^{-1}\cos\omega_i T+e^{-2\sigma_i T}z^{-2}},$$
$$B_{i,s}(z)=\frac{e^{-\sigma_i T}z^{-1}\sin\omega_i T}{1-2e^{-\sigma_i T}z^{-1}\cos\omega_i T+e^{-2\sigma_i T}z^{-2}}, \tag{6}$$

where the impulse responses of $B_{i,c}(z)$ and $B_{i,s}(z)$ are $e^{-\sigma_i t}\cos\omega_i t$ and $e^{-\sigma_i t}\sin\omega_i t$ in continuous-time domain, respectively. The time constant, σ_i, determines the decaying speed of the impulse response and it is an important design parameter affecting the control performance. Two IIR bases, $B_{i,c}(z)$ and $B_{i,s}(z)$ with real coefficients, represent an IIR base with a center frequency ω_i. The overall controller structure from the reference input to the control output using IIR bases is schematically drawn in Fig. 5.

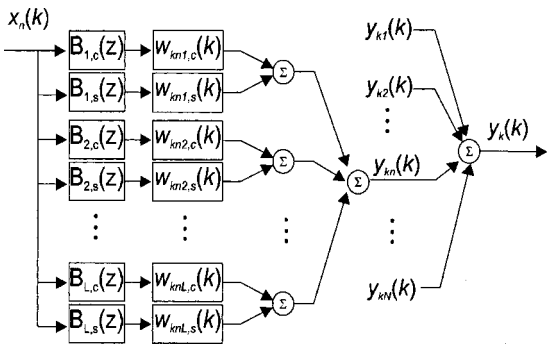

FIG. 5. Controller structure from the nth reference input to control output to the kth secondary source.

Let us define $B_i(z)$ with one pair of base filters as follows:

$$B_i(z)=[B_{i,c}(z)B_{i,s}(z)]^T. \tag{7}$$

To consider L frequency components in the IIR-based filter, there must be L IIR filter bases of Eq. (7).

Denoting $y_{nk}(k)$ as the control output to the kth secondary source due to the nth reference input, $y_k(k)$ can be obtained as the summation of $y_{nk}(k)$ for $n=1,2,...,N$ as follows:

$$y_k(k)=\sum_{n=1}^{N} y_{nk}(k), \tag{8}$$

where

$$y_{nk}(k)=\sum_{i=1}^{L} w_{kni}^T(k)u_{ni}(k), \tag{9}$$

$$w_{kni}(k)=[w_{kni,c}(k)\ \ w_{kni,s}(k)]^T, \tag{10}$$

$$u_{ni}(k)=B_i(z)x_n(k)=[u_{ni,c}(k)\ \ u_{ni,s}(k)]^T. \tag{11}$$

Scalar controller coefficients $w_{kni,c}(k)$ and $w_{kni,s}(k)$ are adaptive weights of $u_{ni,c}(k)$ and $u_{ni,s}(k)$, respectively. $u_{ni}(k)$ is the ith IIR filter output of $x_n(k)$ and its dimension is 2×1—like that of $B_i(z)$.

Because the proposed IIR-based filter does not have any nonlinearity or instability problems on updating the filter weights unlike the conventional adaptive IIR filters, it is easier to model a lightly damped system with an IIR-based filter.

Using this filter instead of an FIR filter, the mth error and constraint error can be written as follows:

$$e_m(k)=d_m(k)=\sum_{n=1}^{N}\sum_{i=0}^{L}\sum_{k=1}^{K}\sum_{j=0}^{L_h} h_{mkj}w_{kni}^T(k-j)u_{ni}(k-j), \tag{12}$$

$$e'_m(k)=d_m(k)+\sum_{n=1}^{N}\sum_{k=1}^{K}\sum_{j=0}^{L_h}\sum_{i=0}^{L} h_{mkj}w_{kni}^T(k)u_{ni}(k-j). \tag{13}$$

The leaky CMFX LMS algorithm with an IIR-based filter that tries to minimize the cost function $e_1'^2(k)+e_2'^2(k)$

TABLE III. Summary of leaky CMFX LMS algorithm with IIR-based filter.

Given $x_n(k), e_m(k), \quad n=1,2,...,N, \quad m=1,2,...,M$ at k step

$$u_{ni}(k)=B_i(z)x_n(k)$$

$$fx_{mkn}(k)=\sum_{j=0}^{L_h} h_{mkj}x_n(k-j)$$

$$fu_{mkni}(k)=B_i(z)fx_{mkn}(k)$$

$$e'_m(k)=e_m(k)-\sum_{k=1}^{K}\sum_{j=0}^{L_h} h_{mkj}y_k(k-j)+\sum_{n=1}^{N}\sum_{k=1}^{K}\sum_{i=0}^{L} w^T_{kni}(k)fu_{mkni}(k)$$

$$w_{kni}(k+1)=(1-\alpha)w_{kni}(k)-2\mu\sum_{m=1}^{M} e'_m(k)fu_{mkni}(k)$$

$$y_k(k)=\sum_{n=1}^{N}\sum_{i=0}^{L} w^T_{kni}(k)u_{ni}(k)$$

$+\cdots+e'^2_M(k)$ is summarized in Table III, and its block diagram is presented in Fig. 6.

The filtered-$u_{ni}(k)$ signal through $H_{mk}(z)$, denoted as $fu_{mkni}(k)$, can be calculated as follows: $fu_{mkni}(k)=H_{mk}(z)u_{ni}(k)=H_{mk}(z)B_i(z)x_n(k)$, but this entails a high computational burden and requires a lot of memory. Since the filters $H_{mk}(z)$ and $B_i(z)$ are linear time-invariant filters, by reversing the filtering order of $H_{mk}(z)$ and $B_i(z)$, $fu_{mkni}(k)$ can be calculated more effectively as $fu_{mkni}(k)=B_i(z)fx_{mkn}(k)$.

V. HARDWARE-IN-THE-LOOP SIMULATION

The locations of the reference accelerometers, error microphones, and control speakers that had been determined in Sec. III were applied to the hardware-in-the-loop simulation and experiment. Two x direction (lateral) acceleration signals from the front wheels were not used on account of the limitation of calculation power, because the lateral motion has minimal correlation with interior noise. Accelerometers were attached symmetrically on the lower arms of front left and right wheels to measure the accelerations of the y and z directions (longitudinal and vertical). Two error microphones were located at the outer ears of two front seats and two commercial loudspeakers were positioned behind the front seats. The control performance is not sensitive to the nearby

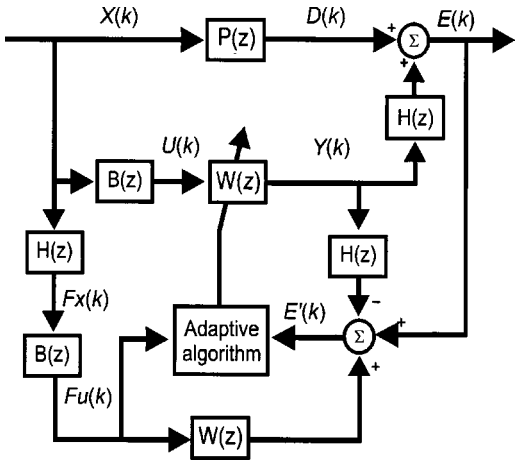

FIG. 6. Block diagram of CMFX LMS algorithm with IIR-based filter.

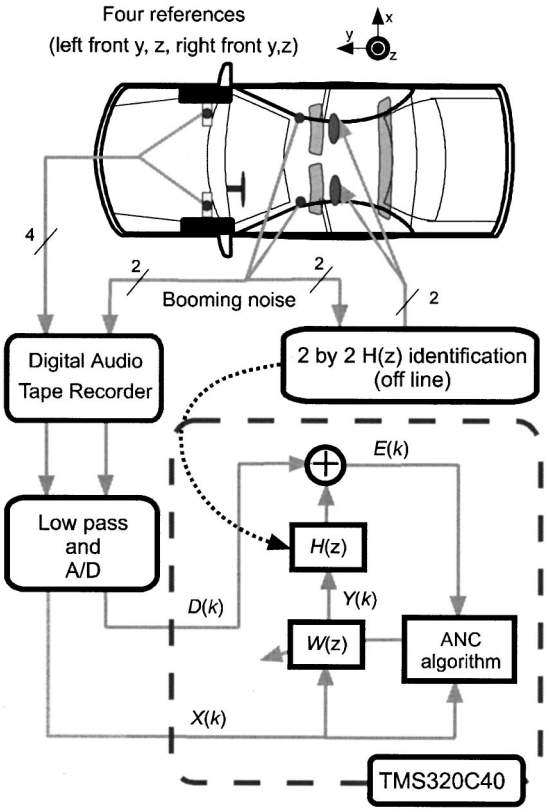

FIG. 7. Experimental setup for hardware-in-the-loop simulation.

change of loudspeaker locations. It can be shifted slightly for manufacturer's convenience. Thus, we developed an ANC system of four references, two secondary speakers and two error microphones, on the test car with the 2000 cc engine. Before carrying out a hardware-in-the-loop simulation, we recorded four accelerations and two error microphone signals while driving on a turtle-back road at a constant speed of 60 km/h. The simulations were carried out playing the record tape. Figure 7 illustrates the overall setup for hardware-in-the-loop simulation. Two microphone signals that are considered as the undesired noises and four reference signals were low-pass-filtered with cut-off frequency of 500 Hz and then A/D converted with a sampling frequency of 1000 Hz. A 2×2 secondary path was identified using two secondary speakers located behind the front seats. We carried out simulations using a DSP board equipped with a TMS320c40 chip.

The lengths of adaptive filters and the secondary path model with FIR type were 130 and 50, respectively. Nine IIR base pairs with center frequencies of 230, 235, 240, 245, 250, 255, 260, 265, and 270 Hz and damping coefficient of $\sigma_i=25$ are selected. IIR bases were concentrated on the road booming noise range.

Figure 8 shows the spectrum of the error microphone signal before and after control at the front right seat while driving on a turtle-back road at a speed of 60 km/h. Every sound pressure spectrum is A-weighted. It is easy to observe that the road booming component appears around 250 Hz from the noise spectrum of ''before control.''

Although the CFX LMS algorithm has better control performance than the conventional FX LMS for this application,[16] little reduction of noise was obtained with the

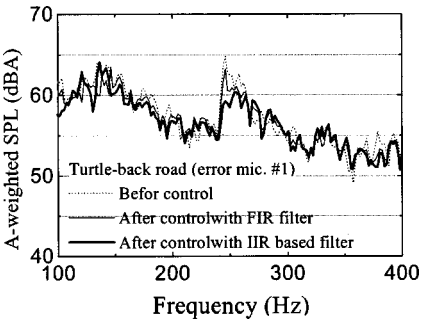

FIG. 8. Hardware-in-the-loop simulation results: Sound pressure level before and after control at the right front error microphone driving on a turtle-back road.

CMFX LMS algorithm while 5 dB of the peak value was reduced using the IIR-based filter in the road booming frequency range. There is no change out of the road booming frequency range when IIR-based filter is used. Driving at constant speed, the road booming noise was still nonlinear (in detail, time varying) because of the road condition, the complexity of suspension, transfer path, and interconnection between the vibration and sound. No reduction can be achieved for a small convergence coefficient with the MFX LMS algorithm and diverged rapidly for a small increment of convergence coefficient even in driving at a constant speed. If the booming noise had been time invariant for a constant driving speed, it could have been reduced with a conventional algorithm. The calculation powers of the two algorithms are almost equal. In this simulation, it is verified that the IIR-based filter is more efficient than an FIR filter for road booming noise which is concentrated in a narrow frequency band.

The length of the adaptive filter could not be increased more than 130 because of the calculation limit of the DSP hardware. For reference, the FIR filter length could be increased up to 300 taps and the reduction of 2 dB at the booming frequency was achieved for one secondary source and one error microphone configuration. The reason for the poor performance of the $4\times2\times2$ CMFX LMS is thought to be the insufficiency of the adaptive filter length. In most discrete-time control systems, the sampling frequency is usually chosen to be ten times the control target frequency for better performance. But in this application, we cannot raise it up over 1000 Hz on account of computation power although the control target frequency was about 250 Hz. Even if the sampling frequency is decreased in order to increase the filter length, the performance will be severely degraded. Reducing the number of filter coefficients while increasing the reference signal also degraded the performance in this simulation. Better performance can hardly be expected with an increasing number of references, as shown in Fig. 3. Another important reason is that the FIR filter tries to reduce error signals with more weighting for higher power components in the least-squares sense. The power of road booming noise under 200 Hz is dominant inside the car, so FIR adaptive filters will try to attenuate these low frequency components first. Since there is little coherence between the references and error signals in this frequency range, the weights of the adaptive filter fluctuate rapidly, thus consuming much of the

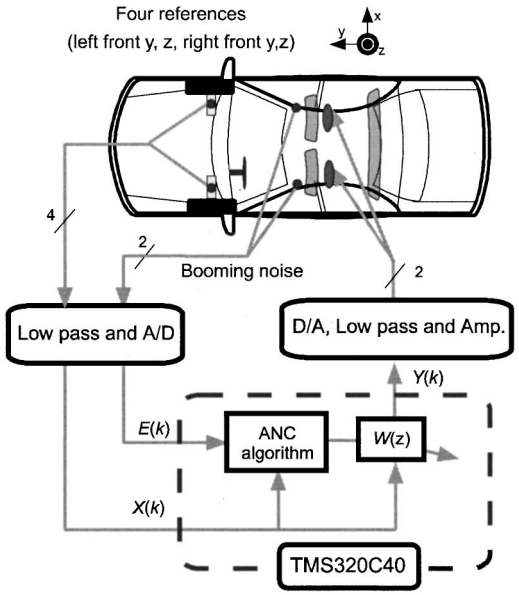

FIG. 9. Experimental setup.

control efforts. The effort to attenuate road booming near 250 Hz is comparatively small despite of higher coherence than in the low frequency range. These make the performance of the CMFX LMS algorithm worse in this application. To enhance the performance using the FIR filter, every reference signal was high-pass filtered, with a cut-off frequency of 150 Hz, and about 2–3 dB reduction of road booming noise was obtained, still below the reduction level of the IIR-based filter.

VI. EXPERIMENT

Real-time experimentation was executed while driving two types of road profiles (rough asphalt road and turtle-back road) at a constant speed of 60 km/h. Performance of the proposed CMFX LMS algorithm using an IIR base filter is compared with that using the conventional FIR filter. Filter length and all other parameters are chosen to be the same in the hardware-in-the-loop simulation for both algorithms. The overall experimental setup is presented in Fig. 9.

The attenuation of overall level of the *A*-weighted spectrums is plotted in Fig. 10. Spectrums of $e(k)$ before control, and after control using the FIR filter and IIR-based one are represented with a dotted line, solid line, and thick solid line, respectively. The conventional CMFX LMS algorithm achieves no remarkable reduction, and even the increment of the noise level is observed for the turtle-back road profile. It is because the signal power of the road booming component in the error microphone signal before *A*-weighting is significantly smaller than that of the noise component under 200 Hz as found in the hardware-in-the-loop simulation. A 5–6 dB reduction was achieved at the two error microphone positions in road booming frequency region near 250 Hz when the IIR-based filter was used. There is no apparent change of noise level out of the booming frequency range where IIR bases are not located. Because of the road booming noise characteristics, the CMFX LMS algorithm using a FIR filter tried to reduce low frequency range and little sound attenu-

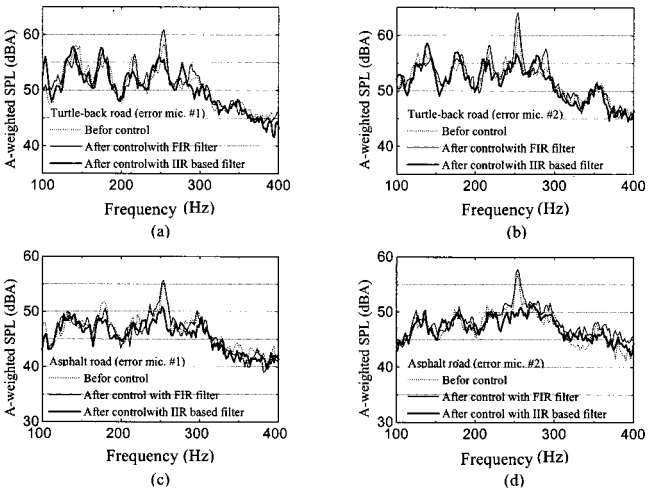

FIG. 10. Experimental results: Sound pressure level before and after control at the (a) right and (b) left error microphone driving on a turtle-back road, at the (c) right and (d) left error microphone driving on an asphalt road at a constant speed of 60 km/h

ation was achieved, whereas the IIR-based filter reduced noise effectively in the range of road booming. The *x* direction accelerometers of the front suspension position ''C'' may give some benefit to the turtle-back road results for 80 and 140 Hz peaks, but if such a reference location is selected, it is hard to expect enhanced control performance for the other road conditions, except for a turtle-back road. Thus, we did not select the *x* direction accelerometers of the front suspension position ''C.'' Road booming noises without/with control for a turtle-back road are greater and harsher than those for a course asphalt road. But the controlled sounds were slightly better than the uncontrolled sounds. Global reduction was not achieved in this study because only two error microphones were attached in front of the car. In order to achieve global reduction, more reference signals detected from the rear suspension system and error microphones would be needed, but the calculation power requirements would be increased substantially.

In this application, the sweet spot is located in a sphere with a diameter of 35–40 cm for 250 Hz noise, so if a driver moves his/her head, he/she can move outside the zone of cancellation with this single-input single-output configuration.

VII. CONCLUSION

Active control of road booming noise using four references, two control speakers, and two error microphones was investigated in the paper. The objective was to attenuate the road booming noise near the headrests of two front seats inside a passenger car. The characteristics of road booming noise of this car were examined and it was found that around 250 Hz was the dominant frequency range of booming noise for the test car. Four reference accelerometers were attached to both sides of the lower arms of the front wheels to maximize the reduction level through multiple coherence analysis. Two loudspeakers were also positioned appropriately to increase the control efficiency considering the primary and secondary paths. A leaky CMFX LMS algorithm with an IIR-based filter was adopted as a fast convergent and efficient algorithm having frequency-selective controllability to reduce time-varying signals effectively. Driving turtle-back and asphalt roads at a constant speed of 60 km/h, a 5–6 dB reduction of road booming noise was achieved at the error microphone positions through the hardware-in-the-loop simulation and experiment with the proposed control system. Comparable reductions could not be obtained with a MFX LMS algorithm or a CMFX LMS algorithm mainly because of the computational power limit. The proposed control system demonstrates the technical feasibility of active control of the road booming noise.

ACKNOWLEDGMENT

This work was financially supported by VRRC (Virtual Reality Research Center) in the ERC program of KOSEF and Brain Korea 21 project of Ministry of Science and Technology, Korea.

[1] B. Widrow and S. D. Stearms, *Adaptive Signal Processing* (Prentice–Hall, New York, 1985).
[2] P. A. Nelson and S. J. Elliott, *Active Control of Sound* (Academic, San Diego, 1992), Chap. 12, pp. 379–407.
[3] C. R. Fuller, S. J. Elliott, and P. A. Nelson, *Active Control of Vibration* (Academic, San Diego, 1996), Chap. 4, pp. 91–111.
[4] S. J. Elliott, I. M. Stothers, P. A. Nelson, A. M. McDonald, D. C. Quinn, and T. J. Saunders, ''The active control of engine noise inside cars,'' in Proceedings of Inter Noise 88, Poughkeepsie, New York, 1988, pp. 987–990.
[5] S. J. Elliott, P. A. Nelson, I. M. Stothers, and C. C. Boucher, ''In-flight experiment on the active control of propeller-induced cabin noise,'' J. Sound Vib. **140**, 219–238 (1990).
[6] C. R. Fuller and J. D. Jones, ''Experiment on reduction of propeller induced noise filed inside flexible cylinder,'' J. Sound Vib. **112**, 389–395 (1987).
[7] R. H. Cabell, H. C. Lester, G. P. Muthur, and B. N. Tran, ''Optimization of actuator arrays for aircraft interior noise control,'' in Proceedings of the Fifteenth AIAA Aeroacoustics Conference, Long Beach, CA, 1993, pp. 93–4447.
[8] A. J. Bullmore, P. A. Nelson, and S. J. Elliott, ''Theoretical studies of the active control of propeller-induces cabin noise,'' J. Sound Vib. **140**, 191–217 (1990).
[9] V. Martin, P. Vignassa, and B. Peseux, ''Numerical vibroacoustic modeling of aircraft for acoustic control of interior noise,'' J. Sound Vib. **176**, 307–332 (1990).
[10] W. Vonheesen, ''Practical experience with an active noise control installation in the exhaust gas line of a cogeneration plant engine,'' Acoustica **82** (Suppl 1), 195 (1996).
[11] S. Kim and Y. Park, ''Active control of multi-tonal noise with reference generator based on on-line frequency estimation,'' J. Sound Vib. **227**, 647–666 (1999).
[12] T. J. Sutton, S. J. Elliott, P. A. Nelson, and I. Moore, ''The active control of road noise inside vehicles,'' in Proceedings of Inter Noise 90, Gothenburg, Sweden, 1990, pp. 1247–1250.
[13] W. B. Ferren and R. J. Bernhard, ''Active control of simulated road noise,'' in Proceedings of the 1991 Noise and Vibration Conference, Traverse City, MI, 1991, pp. 69–82.
[14] T. J. Sutton, S. J. Elliott, A. M. McDonald, and T. J. Saunders, ''The active control of road noise inside vehicles,'' Noise Control Eng. J. **42**, 137–147 (1994).
[15] H. Sano, S. Adachi, and H. Kasuya, ''Active noise control based on RLS algorithm for an automobile,'' in Proceedings of Active 95, Newport Beach, CA, 1995, pp. 891–898.
[16] H.-S. Kim, Y. Park, and K.-H. Sur, ''Active noise control of road booming noise with constraint filtered-X LMS algorithm,'' in Proceedings of Inter Noise 96, Liverpool, UK, 1996, pp. 1155–1158.
[17] C. M. Heatwole, X. Dian, and R. J. Bernhard, ''Determination of the number of input transducers required for active control of road noise in-

side automobiles,'' in Proceedings of Noise-Con 93, Poughkeepsie, New York, 1993, pp. 207–212.
[18] C. M. Heatwole and R. J. Bernhard, ''The selection of active noise control reference transducers based on the convergence speed of the LMS algorithm,'' in Proceedings of Inter Noise 94, Yokohama, Japan, 1994, pp. 1377–1382.
[19] C. M. Heatwole and R. J. Bernhard, ''Reference transducer selection for active control of structure-borne road noise in automobile interiors,'' Noise Control Eng. J. **44**, 35–43 (1996).
[20] W. Dehandschutter and P. Sas, ''Active control of structure-borne road noise using vibration actuators,'' ASME J. Vibr. Acoust. **120**, 517–523 (1998).
[21] M. E. Wang and M. J. Crocker, ''On the application of coherence techniques for source identification in a multiple noise source environment,'' J. Acoust. Soc. Am. **74**, 861–872 (1983).
[22] G. Chen, T. Sone, and M. Abe, ''Effects of multiple secondary paths on convergence properties in active noise control systems with LMS algorithm,'' J. Sound Vib. **195**, 217–228 (1996).
[23] H.-S. Kim and Y. Park, ''A study on performance limit index of feedforward ANC,'' in Proceedings of Korean Society of Noise and Vibration Engineering, Kwang-Ju, Korea, 1995, pp. 161–164.
[24] E. Bjarnson, ''Noise cancellation using a modified form of filtered-X LMS algorithm,'' in Proceedings of Eusipco Signal Processing V, Brussels, Belgium, 1992.
[25] I.-S. Kim, H.-S. Na, K.-J. Kim, and Y. Park, ''Constraint filtered-X and filtered-U least-mean-square algorithm for the active control of noise in ducts,'' J. Acoust. Soc. Am. **95**, 3379–3389 (1994).
[26] H.-S. Na and Y. Park, ''The constraint least mean square error method,'' J. Korean Society of Noise and Vibration Engineering **4**, 59–69 (1994).
[27] H.-S. Na and Y. Park, ''Convergence analysis of the constraint Filtered-X LMS algorithm,'' in Proceedings of Inter Noise 95, Newport Beach, CA, 1995, pp. 485–488.
[28] K. Mayyas and T. Aboulnasr, ''Leaky LMS algorithm: MSE analysis for Gaussian data,'' IEEE SP **45**, 927–934 (1997).
[29] S.-H. Oh and Y. Park, ''Active noise control algorithm using IIR based filter,'' in Proceedings of Inter Noise 98, Christchurch, New Zealand, 1998, pp. 543–546.
[30] S.-H. Oh and Y. Park, ''Active noise control algorithm using IIR based filter,'' J. Sound Vib. **231**, 1396–1412 (2000).